2011 50th IEEE Conference on Decision and Control and
European Control Conference (CDC-ECC)
Orlando, FL, USA, December 12-15, 2011

A Harmonic Potential Field Approach for Planning Motion of a UAV in a Cluttered Environment with a Drift Field

Ahmad A. Masoud
Electrical Engineering, King Fahad University of Petroleum & Minerals, P.O. Box 287, Dhahran 31261, Saudi Arabia,
e-mail: masoud@kfupm.edu.sa

Abstract: This paper tackles motion planning in a cluttered environment with a workspace containing a vector drift field that provides an external influence on the ability of an agent to alter its state. The aim is to develop a planner that can guide the agent to a target zone, avoid clutter and marginalize the influence of drift on motion or exploit its presence in carrying out a task. Here, a variant of the harmonic potential field approach to planning is suggested to jointly process the environment geometry and the drift field and produce a dense, vector field that can safely guide motion from anywhere in the workspace to the target while managing the presence of drift in the desired manner. The approach is developed and its capabilities are demonstrated using simulation. A provably-correct method is also presented for converting the planning action into an equivalent navigation control that suits a wide class of UAVs.

I. Introduction:

A planner is a context-sensitive, goal-oriented, constrained intelligent controller that is required to provide action instructions (control signal) to an agent on how to deploy its actuators of motion so that the target may be reached in a desired manner. A multitude of issues have to be tackled in order for a planner to function in the above capacity. One of these issues has to do with increasing the diversity of environment-related, operator-supplied information which the planner is capable of processing to yield the guidance signal. The overwhelming majority of planners rely solely on the geometry of the environment as the only form of information which the planner is required to process [1,2,3]. This geometry usually describe a binary partition of the environment consisting of forbidden regions which the agent should avoid (obstacles) and admissible regions which the agent is allowed to operate in (workspace). Occasionally a workspace contains a force external to the agent that influences its state. This force is known as the drift field. A drift field is usually treated as a source of disturbance whose influence should be suppressed by the agent's low-level controller. With the advances in forecast technology [4] a drift field may be predicted for a considerable period of time making it a source of information which should be incorporated in the generated plan instead of being a source of disturbance that has to be suppressed. This is finding important applications in planning for energy-exhaustive missions where good planning does not only reduce the energy drain caused by drift, but may even use it as a source for powering the agent. For example, it is desirable to move a UAV aerial glider along a path where the lift component of the drift field (wind) is highest [5,23]. A path planned for an autonomous under water vehicles (AUV) operating in littoral water should be laid where the energy drain experienced due to water current is minimized [6].

Several techniques were suggested for incorporating drift fields in the planning process. Most of these techniques use optimization or search-based methods for determining the minimum cost path that connects two points in the drift-occupied space while avoiding the obstacles. In [6] a genetic algorithm planner is used to lay a minimum energy trajectory for an AUV operating in turbulent waters. A tree-based planner [7] was used to lay a path for an aerial glider along the component of wind having maximum lift. The A* search approach is used for planning a path for an AUV operating in a current field [8]. A symbolic wave expansion approach is developed to tackle planning in workspaces with dynamic current fields [9]. Other approaches may be found in [5,10]. This work extends the capabilities of the harmonic potential field (HPF) planning approach [11,12,13] to accommodate a drift field as an external source of information. The HPF approach has several advantages: it can easily generate a well-behaved control signal for both holonomic [14,15] and nonholonomic robots [16]. It is capable of integrating a variety of constraints in the planning process [17] as well as take the ambiguity of data into account [18]. The approach can be easily configured in a multi-agent mode [19]. Adding the ability to incorporate drift fields in the HPF planner will further enhance such type of planners' ability to function as a part of an integrated system [20] that has a reasonable chance of projecting successful behavior in a realistic environment.

This paper is organized as follows: in section II the planning task is stated. In section III the modified, drift-sensitive, HPF planner is developed. Section IV suggests a procedure for utilizing the planner with a discrete-in-time sequence of drift field templates. In section V converting the guidance signal into a control signal is discussed. Section VI contains simulation results and conclusions are placed in section VII.

II. Problem Statement.

The planner suggested in this paper is a gradient dynamical system of the form:

$$\dot{\mathbf{X}} = -\nabla \mathbf{V}(\mathbf{X}) \tag{1}$$

The solution of such a system (i.e. generated trajectory) is required to satisfy the following conditions

$$\begin{aligned} &\lim_{t\to\infty} \mathbf{X(t)} \to \mathbf{X_T}\ , \qquad \forall \mathbf{X(0)} \in \Omega \\ &\mathbf{X(t)} \cap \mathbf{O} \equiv \phi \qquad \forall \mathbf{t} \qquad \textbf{and} \\ &\mathbf{U} = \int_0^\infty \mathbf{Fc}(\Psi(\mathbf{X(t)}), -\nabla \mathbf{V}(\mathbf{X(t)}))\left|\nabla \mathbf{V}(\mathbf{X(t)})\right| \mathbf{dt} \end{aligned} \tag{2}$$

is minimized (or reduced to a satisfactory value); where $X \in R^N$, O is the set of forbidden regions (obstacles, $\Gamma=\partial O$), Ω is the subset of admissible space (worksapce), $\Psi()$ is the field in Ω describing drift, U is a task-related cost functional constructed

by accumulating point costs (Fc(X)) along the path of the agent from the starting point to the target and Fc is a point cost function constructed in aim with the aspect of interest to the operator. This function is dependant on the direction along which motion is heading relative to that of the drift field. Fc is constructed based on the mission that is being planned for. In an energy exhaustive mission it is desirable that the obstacle-free path connecting the start and end points together has a drift component that is in-phase with the direction along which motion is heading. A choice of Fc is

$$\mathbf{Fc} = \frac{\mathbf{K}}{\mathbf{2}}(1-\cos(\Theta)) = \frac{\mathbf{K}}{\mathbf{2}}(\mathbf{1}+\frac{\nabla\mathbf{V}^{\mathbf{T}}\Psi}{|\nabla\mathbf{V}||\Psi|}), \tag{3}$$

and $$\mathbf{Fu} = \mathbf{K} - \mathbf{Fc} = \frac{\mathbf{K}}{\mathbf{2}}(\mathbf{1}-\frac{\nabla\mathbf{V}^{\mathbf{T}}\Psi}{|\nabla\mathbf{V}||\Psi|}).$$

where Θ is the angle between $-\nabla V$ and Ψ, K is a positive constant and Fu is a function describing the utility of the drift at a certain point in space.

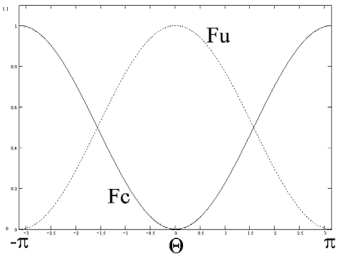

Figure-1: The suggested utility function versus Θ.

To empower an agent to carry-out the task encoded in the gradient field, $-\nabla V(X)$ has to be converted into a control signal that is capable of making the dynamical trajectory of the system in (4) coincide with the kinematic trajectory generated by the gradient system in (1)

$$\begin{aligned} \dot{\mathbf{X}} &= \mathbf{G}(\lambda) \\ \dot{\lambda} &= \mathbf{F}(\lambda, \mathbf{u}) \end{aligned} \tag{4}$$

where G is an orthogonal coordinate transformation, λ is the local coordinates of the agent and F describes the manner in which motion is actuated in the local coordinates of the agent. The system in (4) covers a large variety of practical agents such as a fixed wing aircraft whose model is shown in (5)

$$\begin{aligned} \dot{\mathbf{x}} &= \nu\cdot\mathbf{cos}(\gamma)\mathbf{cos}(\psi) \\ \dot{\mathbf{y}} &= \nu\cdot\mathbf{cos}(\gamma)\mathbf{sin}(\psi) \\ \dot{\mathbf{z}} &= \nu\cdot\mathbf{sin}(\gamma) \\ \dot{\nu} &= \frac{\mathbf{F_T}}{\mathbf{M}} - \mathbf{g}\cdot\mathbf{sin}(\gamma) \\ \dot{\gamma} &= \frac{\mathbf{F_N}\cdot\mathbf{cos}(\sigma)}{\mathbf{M}\cdot\nu} - \mathbf{g}\frac{\mathbf{cos}(\gamma)}{\nu} \\ \dot{\psi} &= \frac{\mathbf{F_N}\cdot\mathbf{sin}(\sigma)}{\mathbf{M}\cdot\nu\cdot\mathbf{cos}(\gamma)}. \end{aligned} \tag{5}$$

$F_T = T\cdot\cos(\epsilon) - D, \qquad F_N = T\cdot\sin(\epsilon) + L$

$$\mathbf{D} = \frac{\mathbf{C_D}}{\mathbf{2}}\rho\nu^2, \qquad \mathbf{L} = \frac{\mathbf{C_L}}{\mathbf{2}}\rho\nu^2$$

were ν is the tangential speed of the UAV, γ is flight path angle, ψ is directional angle, σ is the banking angle, ϵ is the angel of attack, M is the point mass of the UAV, F_T is the resultant force along the velocity vector, F_N is the resultant force normal to the velocity vector, g is the constant of gravity, T is the thrust from the UAV engine, D is the aerodynamic drag, L is the aerodynamic lift, C_L, C_D are positive constants, ρ is air density and λ is a vector describing motion in the local coordinates of the UAV, $X=[x\ y\ z]^t$, $\lambda=[\nu\ \gamma\ \psi]^t$.

In the following section the harmonic potential field approach to planning is modified to address the planning task in (2). The HPF approach belongs to the family of partial differential equation -ordinary differential equation (PDE-ODE) planners (figure-2)[21]. The ODE part is similar to the one in (1). The focus is on developing the PDE that encodes the desired behavior in the potential in a manner that is retrievable by its gradient field.

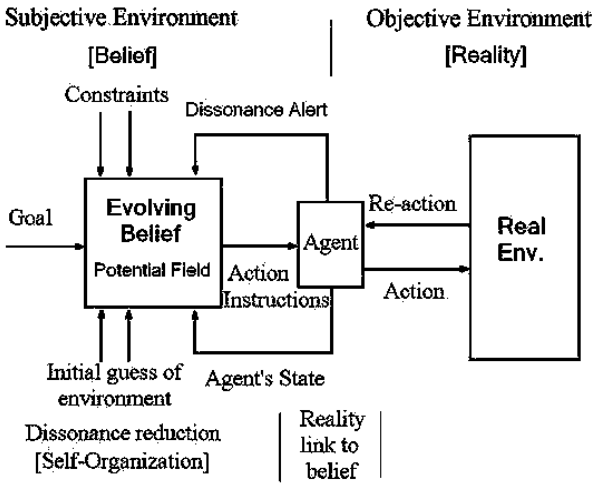

Figure-2: Structure of a Hybrid PDE-ODE planner.

III. The Suggested extension :

A constructive metaphor for understanding the HPF approach is that of an electric current flowing in a homogeneous conductor (figure-3) having a conductivity $\sigma(X)$ [22]. The conductor has insulators ($\sigma=0$) occupying the forbidden regions surrounded by Γ.

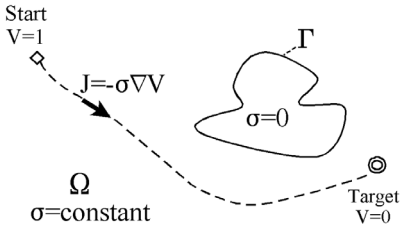

Figure-3: Physical metaphor for the planner

This analogy was recently used by the author [18, 24] to develop a provably-correct variant of the HPF approach. The approach uses a descriptor ($\sigma(X)$) that marks at each point in the agent's space the agent's ability to perform an assigned task. The approach is called the G-Harmonic potential planner. The modified PDE part of the HPF planner is obtained as

$$\nabla\cdot(\sigma(X)\nabla V(X)) \equiv 0 \qquad X\in\Omega \tag{6}$$

subject to: $V(X_S) = 1$, $V(X_T) = 0$, and $\frac{\partial V}{\partial \mathbf{n}} = 0$ at $X = \Gamma$.

A provably-correct path may be generated (figure-4) using the gradient dynamical system:

$$\dot{x} = -\nabla V(x). \qquad (7)$$

such that $\lim_{t\to\infty} \mathbf{x}(t) \to \mathbf{x}_T$, $\forall \mathbf{x}(0) \in \Omega$

$\mathbf{x}(t) \cap \mathbf{O} \equiv \phi \qquad \forall t$

where Ω is the workspace, Γ is its boundary, $\mathbf{n}$ is a unit vector normal to Γ, X_s is the start point, X_T is the target point and O is the set of zero fitness regions in the agent space (O={X: σ(X)=0}). As a direct consequence of the analogy with the electric current, the trajectory generated minimizes the total risk of moving to the target.

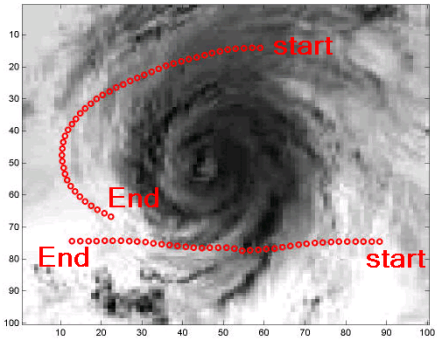

Figure-4 trajectories from the G-harmonic planner.

Note that σ and Fu have the same nature in terms of measuring the fitness of the trajectory to pass through a point x in the workspace. Replacing σ with Fu in the differential operator in (6) yields:

$$\nabla \cdot (\frac{\mathbf{K}}{2}(\mathbf{1} - \frac{\nabla \mathbf{V}^{\mathbf{T}} \Psi}{|\nabla \mathbf{V}||\Psi|})\nabla \mathbf{V}) \equiv \mathbf{0}, \qquad (8)$$

which reduces to:

$$\nabla^2 \mathbf{V} - \nabla \cdot (\frac{\nabla \mathbf{V}^{\mathbf{T}} \Psi}{|\nabla \mathbf{V}||\Psi|})\nabla \mathbf{V}) \equiv \mathbf{0}. \qquad (9)$$

The overall PDE component of the planner is:

$$\nabla^2 \mathbf{V} - \nabla \cdot (\frac{\nabla \mathbf{V}^{\mathbf{T}} \Psi}{|\nabla \mathbf{V}||\Psi|})\nabla \mathbf{V}) \equiv \mathbf{0}. \quad X \in \Omega \qquad (10)$$

subject to: $V(X_S) = 1$, $V(X_T) = 0$, and $\frac{\partial V}{\partial \mathbf{n}} = 0$ at $X = \Gamma$,

The path may be generated using the dynamical system in (1). The proof of the ability of the planner in (10) to converge to the target from anywhere in Ω and avoid forbidden regions follows closely the proofs in [18,24]. As for minimizing the value of U or reducing it to an acceptable level, it is expected to be mathematically involved and for now it is demonstrated by simulation.

A way for avoiding the forbidden regions (obstacles, O) is to force the value of the utility function (Fu) to zero in O. This leads to the generating PDE

$$\nabla^2 \mathbf{V} - \nabla \cdot (\frac{\nabla \mathbf{V}^{\mathbf{T}} \Psi}{|\nabla \mathbf{V}||\Psi|})\nabla \mathbf{V}) \equiv \mathbf{0}. \quad X \in \Omega \qquad (11)$$

subject to: $V(X_S) = 1$, $V(X_T) = 0$, and $Fu \equiv 0$ at $X \in O$,

Same as before, the path may be generated using the dynamical system in (1). Proofs of convergence an avoidance follow closely the proofs in [18,24].

IV. Extension to a sequence of drift field templates

In this section a heuristic procedure is suggested for utilizing the planner for generating a path when a discrete time sequence of drift fields is supplied. The approach is based on proceeding along the lowest cost trajectory generated by the system in (10) while respecting the temporal sequencing of the navigation policies.

Let a drift field forecast yield a sequence of N vector fields

$$\Psi_i(X) \qquad i=1..N \qquad (12)$$

where the i'th field template ($\Psi_i(X)$) exist in the time period $t=[T_i, T_{i+1})$, $T_0=0$ and $T_{N+1}\to\infty$. Also, let the navigation policy $-\nabla V_i$ correspond to the i'th drift field template. Let $\rho_i(p)$ be the trajectory generated by $-\nabla V_i$ from the starting point p and let $U_i(p)$ be the cost function computed along the trajectory $\rho_i(p)$ from the starting point p to the target point x_T. Let a breakaway point β_k be defined as the point where the cost of proceeding towards the target using the path generated by a future navigation policy becomes lower than that of the one that can be achieved by the currently used navigation policy ($U_i(\beta_k) > U_j(\beta_k)$, j>i). The procedure for generating the path (figure-5) from multiple navigation policies is

1- generate the navigation policies ($-\nabla V_i$) independently for each $\Psi_i(X)$
2- initialize $\beta_0 = X_s$
3- using the gradient dynamical systems:

$$\dot{\mathbf{X}} = -\nabla V_i(\mathbf{X}). \quad X(0)=\beta_0 \quad i=1,..N \qquad (13)$$

generate $\rho_i(\beta_0)$ and compute $U_i(\beta_0)$,
4- select the navigation policy $-\nabla V_j$ for generating the trajectory $\rho_j(\beta_0)$ where ($U_i(\beta_0) \geq U_j(\beta_0)\ \forall\ i \neq j$)
5- move along $\rho_j(\beta_0)$ checking at each point on the trajectory the value of the cost function $U_j(\rho_j(\beta_0))$ with respect to cost functions generated by future navigation polices $U_k(\rho_j(\beta_0))$ k>j.
6- if a point is encountered where $U_j(\rho_j(\beta_0)) > U_k(\rho_j(\beta_0))$ set that point as a BAP (β_1) and start generating the trajectory using the dynamical system

$$\dot{\mathbf{X}} = -\nabla V_k(\mathbf{X}). \quad X(0)=\beta_1 \qquad (14)$$

7- repeat the above until the target is reached.

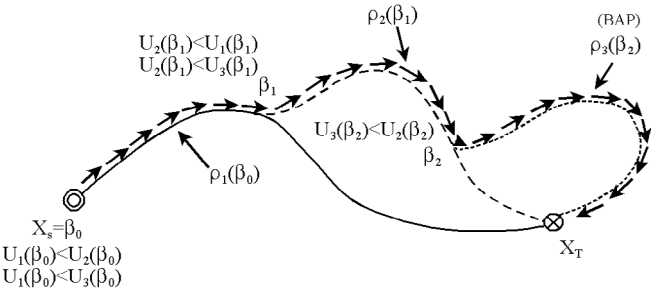

Figure-5: Path from multi-template drift field.

V. Control signal generation

In a recent work, the author suggested a novel approach for converting, in a provably-correct manner, the guidance field from a harmonic potential into a control field that suits an agent

whose system equation can be expressed in the form in (4) [25,26]. To perform simultaneous planning and control, the approach treats the control signal as a fictitious state hence unifying the state variables and control variables in one hyper state space system (15)

$$\begin{bmatrix} \dot{\mathbf{X}} \\ \dot{\lambda} \\ \dot{\mathbf{u}} \end{bmatrix} = \begin{bmatrix} \mathbf{G}(\lambda) \\ \mathbf{F}(\lambda,\mathbf{u}) \\ \mathbf{Q}(\mathbf{X},\lambda,\mathbf{u}) + \chi(u) \end{bmatrix} \quad (15)$$

where $\mathbf{Q}(\mathbf{X},\lambda,\mathbf{u}) = \mathrm{K_u}\mathbf{J_u^T}\left[\mathrm{K}_\lambda \mathbf{J}_\lambda^{\mathrm{T}}(-\nabla\mathbf{V}(\mathbf{X}) - \mathbf{G}(\lambda)) - \mathbf{F}(\lambda,\mathbf{u})\right]$, $\mathrm{K_u}$, K_λ are positive constants,

$$\mathbf{J_u} = \frac{\partial \mathbf{F}(\lambda,\mathbf{u})}{\partial \mathbf{u}}, \quad \mathbf{J}_\lambda = \frac{\partial \mathbf{G}(\lambda)}{\partial \lambda} \quad (16)$$

and χ(u) is a barrier function used to constrain the magnitude of the control signal

$$\chi(\mathbf{u}) = \sum_{i=1}^{M} \chi_i(\mathbf{u}_i) \qquad \chi_i(\mathrm{u}) = \begin{bmatrix} -\mathbf{K} & \mathbf{u_i} = \mathbf{u_i^+} \\ +\mathbf{K} & \mathbf{u_i} = \mathbf{u_i^-} \\ \mathbf{0} & \mathbf{elsewhere} \end{bmatrix} \quad \mathrm{i}=1,..,\mathrm{M} \quad (17)$$

where $\mathrm{u_i^+}$, $\mathrm{u_i^-}$ are the upper and lower bounds on $\mathrm{u_i}$ respectively and K is a positive constant. The control signal is generated as

$$\mathbf{u(t)} = \int_{\mathbf{t_0}}^{\mathbf{t}} \dot{\mathbf{u}} d\mathbf{t} \quad (18)$$

The suggested structure for joint planning and control is shown in figure-6

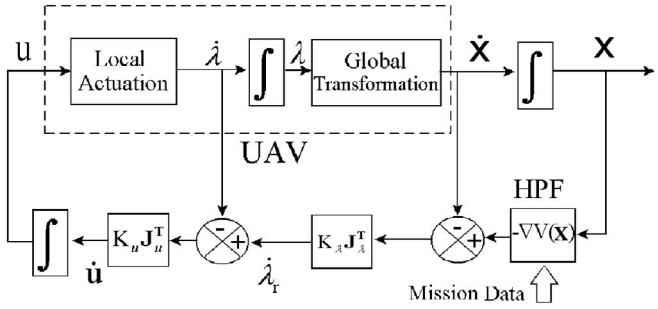

Figure-6: The joint planning and control structure.

One can show if the condition $\mathbf{K} \geq \underset{\mathbf{x},\lambda,\mathbf{u}}{\mathbf{Max}} |\mathbf{Q}(\mathbf{x},\lambda,\mathbf{u})|$ is satisfied the system in (15) is stable and satisfies the conditions in (19)

$$\underset{\mathbf{t}\to\infty}{\mathbf{Lim}}\, \mathbf{x(t)} \to \mathbf{x_T} \qquad \mathbf{u_i^-} < \mathbf{u(t)} < \mathbf{u_i^+} \quad i = 1,..,L \quad (19)$$

One can also show that all the properties encoded in the gradient navigation field will be migrated to the control signal. In other words, if the initial error between the dynamic trajectory ρ_d

$$\rho_d = \{\mathbf{X(t)}: \begin{bmatrix} \dot{\mathbf{X}} \\ \dot{\lambda} \\ \dot{\mathbf{u}} \end{bmatrix} = \begin{bmatrix} \mathbf{G}(\lambda) \\ \mathbf{F}(\lambda,\mathbf{u}) \\ \mathbf{Q}(\mathbf{X},\lambda,\mathbf{u}) \end{bmatrix}\} \quad (20)$$

and the kinematic trajectory ρ_k

$$\rho_\mathrm{k} = \{\mathbf{X(t)}: \dot{\mathbf{X}} = -\nabla\mathbf{V}(\mathbf{X})\}\,. \quad (21)$$

is zero, then $\rho_\mathrm{d} = \rho_\mathrm{k}$ $\forall$t.

VI. Simulation Results

In this section the ability of the planner to process the drift data and the geometry of the space and generate a well-behaved navigation policy and trajectory is demonstrated for different drift scenarios.

In figure-7 the planner tackles a drift that has a vortex form and is rotating in a counter clockwise direction. The drift is restricted to a closed square environment. The graph in figure-7 shows both the generated path and the drift field.

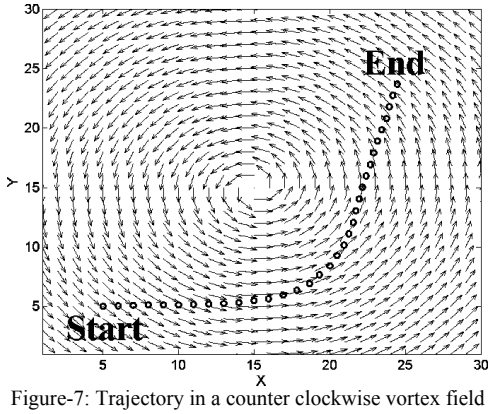

Figure-7: Trajectory in a counter clockwise vortex field

The navigation policy responsible for generating the path is shown in figure-8. The corresponding harmonic potential generating the policy is shown in figure-9 and the point utility function for the drift is shown in figure-10.

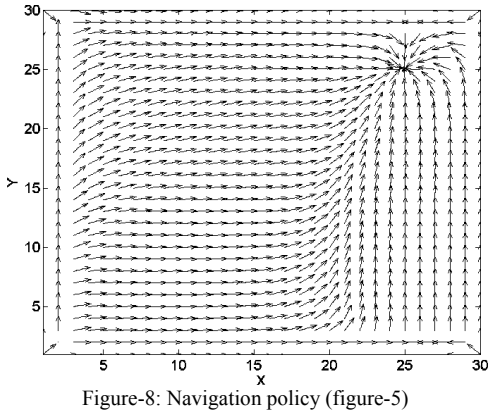

Figure-8: Navigation policy (figure-5)

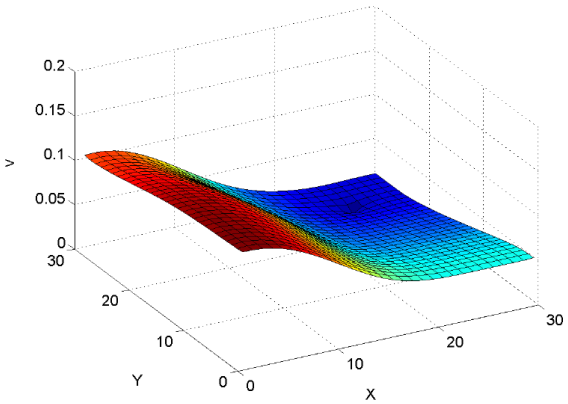

Figure-9: Potential field (figure-5).

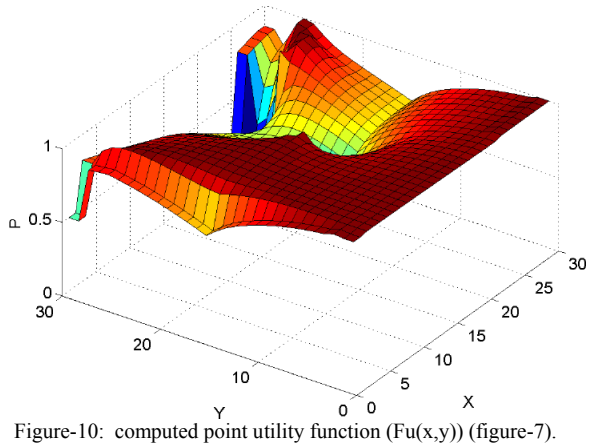

Figure-10: computed point utility function (Fu(x,y)) (figure-7).

In figure-11, the direction of rotation of the vortex drift is reversed. As can be seen the planner responded by selecting a path to the target that moves with the flow, has a reasonable length and is sensitive to the confines in which it is operating.

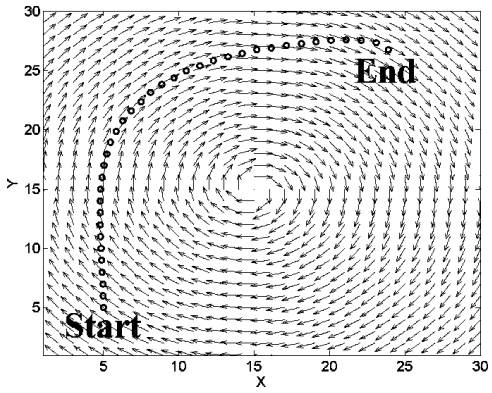

Figure-11: Trajectory in a clockwise vortex field

In figure-12 a random correlated drift field is used instead of the vortex field. As can be seen a smooth and safe path with reasonable length was laid to the target. As can be seen from figure-13, it was possible to lay the path so that most of the drift field components along it aid motion. The navigation policy, figure-14, is smooth despite the fact that the information being processed is random.

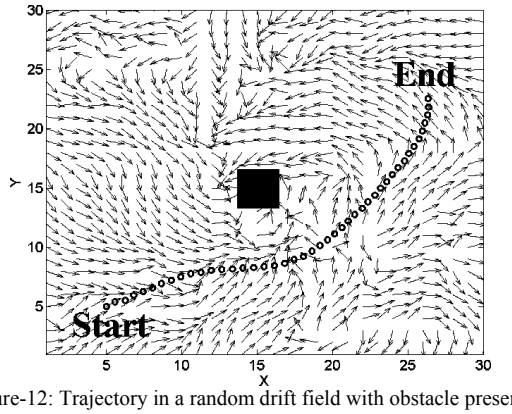

Figure-12: Trajectory in a random drift field with obstacle present.

In figure-15 the workspace contains a variable drift consisting of two successive templates Ψ1 and Ψ2 selected as the vortex fields in figures-7,11. At each point on the path generated by the first template (Ψ1) the cost is compared to the path generated by Ψ2. It is noticed that the cost of proceeding to the target along the path generated by Ψ1 is always less than that of proceeding to the target along the path generated by Ψ2. According to the procedure in IV, the path generated by Ψ1 from start to end is selected as the whole path. This implies that the agent must adjust its speed so that the whole path is traveled during the time for which Ψ1 is present. Had the path generated by Ψ2 being the lower cost path, the agent will have to wait at the start point till Ψ1 is over then start moving towards the target. The procedure in IV will have to modified if time constraints on the speed of the agent are imposed. The selected path is shown in figure-16.

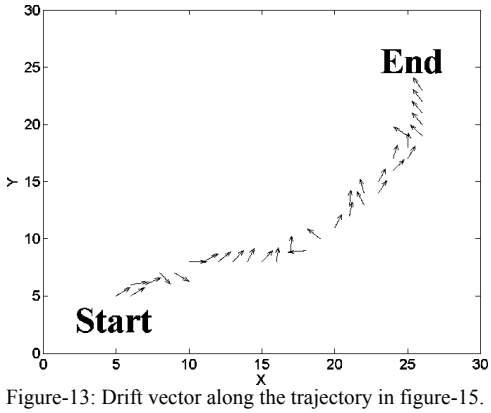

Figure-13: Drift vector along the trajectory in figure-15.

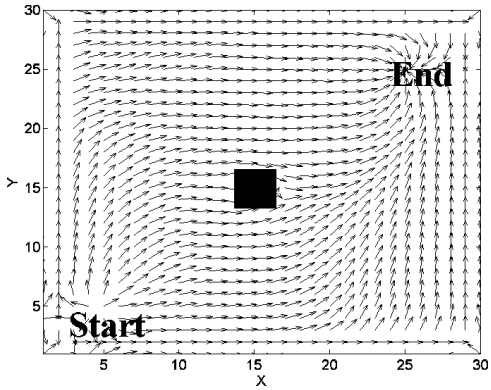

Figure-14: The guidance policy corresponding to figure-12.

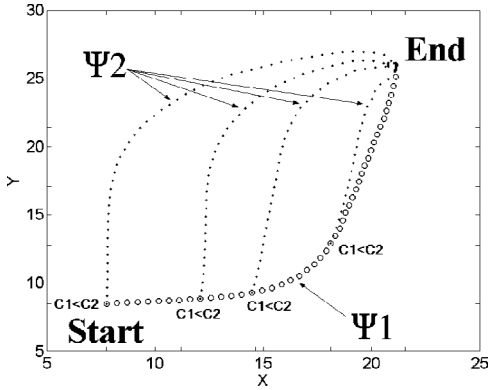

Figure-15: path from two oppositely circulating vortex drift templates.

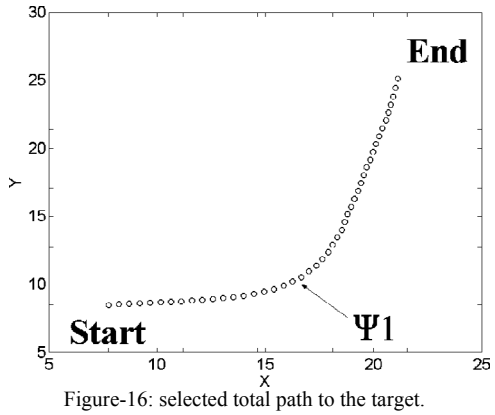

Figure-16: selected total path to the target.

The following example demonstrates the ability to convert the gradient guidance field into a navigation control field for an involved nonlinear agent. The method reported in [25,26] is used for such a purpose. The system for which joint planning and control is carried out is the spherical system with redundant actuation shown in (22)

$$\begin{aligned} \dot{x} &= \nu \cdot C\varphi C\theta \\ \dot{y} &= \nu \cdot S\varphi S\theta \\ \dot{z} &= \nu \cdot C\theta \\ \dot{\nu} &= u_1 \cdot u_4 \\ \dot{\theta} &= \cos(u_2) + u_3^2 + u_5 \\ \dot{\varphi} &= \cos(u_2)\sin(u_4) + u_6 \end{aligned} \quad . \qquad (22)$$

An opportunistic navigation control is to be synthesized for the system in (22) in 3D from a start to an end point. The agent is required to climb up to an altitude z=2 and move in the xy plane from start to end while making use of the drift field in the environment. The field is shown in figure-17 superimposed on an intensity map where the brighter the map, the stronger the drift.

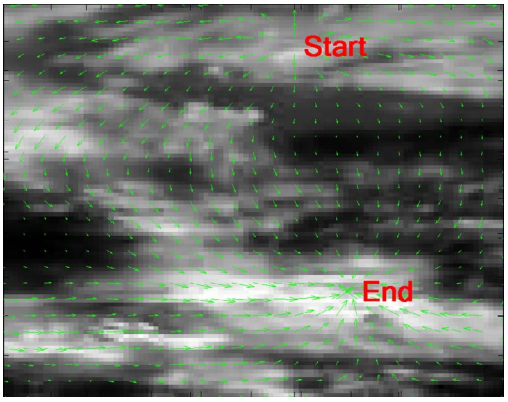

Figure-17: the xy drift map.

The generated dynamical, 3D trajectory is shown in figure-18. As can be seen the controller manages to drive the agent from start to end while maintaining the desired elevation along a well-behaved trajectory. The xy projection of the trajectory (figure-19) clearly shows that the path selected is always along a high drift field component. It also clearly shows that the dynamical trajectory (solid red) is very close the kinmatic trajectory (dotted blue) that is generated by the guidance gradient field.

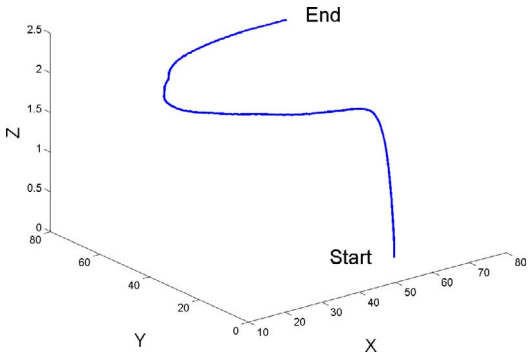

Figure-18: the 3D dynamical trajectory.

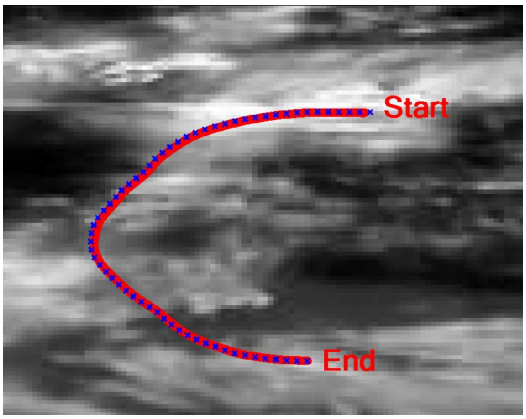

Figure-19: xy projection of the trajectory.

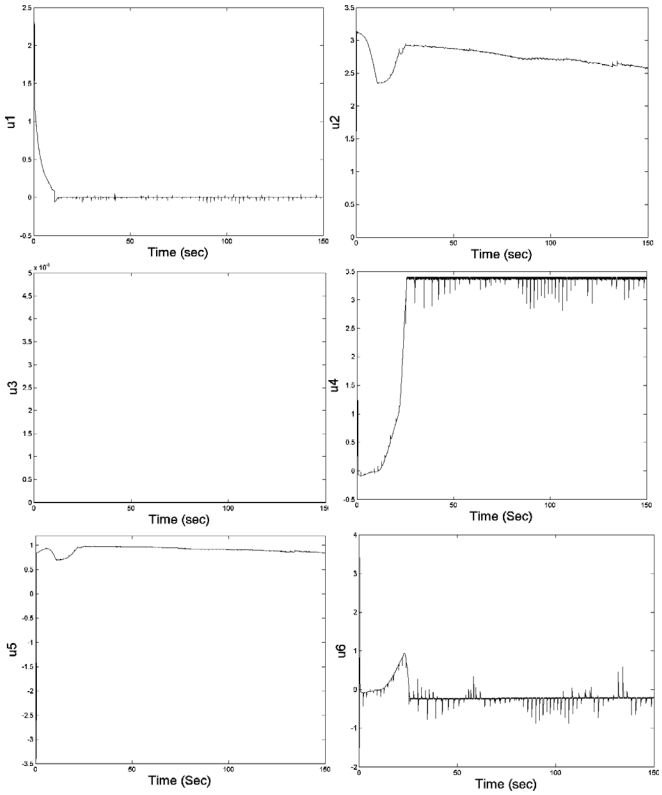

Figure-20: the navigation control signals.

The six navigation control signals are shown in figure-20. As can be seen the signals are well-behaved. It is worth mentioning that the control signals were constrained so that their magnitude does not exceed a certain value. Constraints in the control space were enforced with no effect on the ability of the planner to steer motion in accordance with the desired aim.

VII. Conclusion

In this paper the capabilities of the HPF approach are extended to tackle planning in an environment with a cluttered workspace that is populated by a drift field. The suggested extension along with the means for performing simultaneous planning and control is a proof of principle that the HPF approach is capable of efficiently addressing the information diversity issue needed for a planner to tackle a realistic situation. Although the presentation in the paper mainly aims at developing the new HPF-based approach and demonstrating its capabilities with no mathematical proofs provided at this stage, the approach is a provably-correct in terms of its ability to converge to the target and avoid cluttered regions. It ought to be noticed that in achieving the above objective the modified approach retains all the desired aspects of an HPF-based generated trajectory. The generated path is smooth even when the information being processed have a random nature. This also applies to the navigation policy which is both smooth and guarantees convergence to the target from anywhere in the workspace. As a result it is possible to use the approaches in [16,25,26] for converting the guidance signal into a well-behaved control signal. The paths generated also have a reasonable length and are dynamically friendly. This author strongly believe that the suggested approach is another firm step towards developing an integrated planner that has a reasonable chance of success operating in a realistic environment.

Acknowledgment: The author would like to thank King Fahad University of Petroleum and Minerals (KFUPM) for its support of this work.

References:

[1] B. Siciliano, O. Khatib, “Handbook of Robotics”, Springer-Verlag, Berlin Heilderberg, 2008

[2] S. LaValle, “Planning Algorithms”, Cambridge University Press, 2006

[3] H. Choset, K. Lynch, S. Hutchinson, G. Kantor, W. Burgard, L. Kavraki, S. Thrun, "Principles of Robot Motion: Theory, Algorithms and Implementation", A Bradford Book, the MIT Press, Cambridge, Massachusetts, London England, 2005.

[4] J. Scott Armstrong, “Long-Range Forecasting”. John Wiley 1985. Second Edition

[5] Juan Carlos Rubio, Sean Kragelund, "The Transpacific Crossing: Long Range Adaptive Path Planning for UAVS Through Variable Wind Fields", Digital Avionics Systems Conference, 2003. DASC '03. The 22nd Publication Date: 12-16 Oct. 2003 Volume: 2, On page(s): 8.B.4- 81-12 vol.2.

[6] A. Alvarez, A. Caiti, R. Onken, "Evolutionary Path Planning for Autonomous Underwater Vehicles in a Variable Ocean", IEEE Journal of Oceanic Engineering, vol. 29, no. 2, April 2004, pp. 418-429

[7] Jack W. Langelaan, "Tree-based Trajectory Planning to Exploit Atmospheric Energy", 2008 American Control Conference, Westin Seattle Hotel, Seattle, Washington, USA, June 11-13, 2008

[8] Bartolome Garau, Alberto Alvarez, Gabriel Oliver, "Path Planning of Autonomous Underwater Vehicles in Current Fields with Complex Spatial Variability: an A* Approach", Proceedings of the 2005 IEEE, International Conference on Robotics and Automation Barcelona, Spain, April 2005

[9] M. Soulignac, P. Taillibert, M. Rueher, "Time-minimal Path Planning in Dynamic Current Fields", 2009 IEEE International Conference on Robotics and Automation, Kobe International Conference Center, Kobe, Japan, May 12-17, 2009

[10] Hiroshi Kawano,, "Method for Designating the Wind Condition in MDP-based Motion Planning of Under-actuated
Blimp type UAV", 2007 IEEE International Conference on Robotics and Automation Roma, Italy, 10-14 April 2007.

[11] K. Sato,”Collision Avoidance in Multi-dimensional Space Using Laplace Potential”, Proc. 15th Conf. Rob. Soc. Jpn., 1987, pp.155- 156.

[12] C. Connolly, R. Weiss, J. Burns,”Path Planning using Laplace Equation”, 1990 IEEE International Conference on Robotics and Automation, May 13-18, 1990, Cincinnati, Ohio, pp. 2102-2106.

[13] D. Keymeulen, J. Decuyper,” A Reactive Robot Navigation System Based on a Fluid Dynamics Metaphor”, AI MEMO # 90-5, Artificial Intelligence Lab., Vrije Universiteit Brussel, 1990.

[14] S. Masoud Ahmad A. Masoud, "Constrained Motion Control Using Vector Potential Fields", The IEEE Transactions on Systems, Man, and Cybernetics, Part A: Systems and Humans. May 2000, Vol. 30, No.3, pp.251-272.

[15] A. Masoud, "Kino-Dynamic, Harmonic, Potential Field- based Motion Planning Using Nonlinear Anisotropic Damping Forces", to appear in the: IEEE Robotics and Automation Magazine.

[16] A. Masoud, "A Harmonic Potential Field Approach for Navigating a Rigid, Nonholonomic Robot in a Cluttered Environment", 2009 IEEE International Conference on Robotics and Automation, May 12 - 17, 2009, Kobe, Japan. pp. 3993-3999.

[17] S.. Masoud, Ahmad A. Masoud, " Motion Planning in the Presence of Directional and Obstacle Avoidance Constraints Using Nonlinear Anisotropic, Harmonic Potential Fields: A Physical Metaphor", the IEEE Transactions on Systems, Man, & Cybernetics, Part A: systems and humans. Vol 32, No. 6, November 2002, pp. 705-723.

[18] A. Masoud, "A Harmonic Potential Field Approach with a Probabilistic Space Descriptor for Planning in Non-divisible Environments.", 2009 IEEE International Conference on Robotics and Automation, May 12 - 17, 2009, Kobe, Japan. 3774-3779.

[19] A. Masoud, "Decentralized, Self-organizing, Potential field-based Control for Individually-motivated, Mobile Agents in a Cluttered Environment: A Vector-Harmonic Potential Field Approach", IEEE Transactions on Systems, Man, & Cybernetics, Part A: systems and humans, Vol. 37, No. 3, pp. 372-390, May 2007.

[20] R. Gupta, A Masoud, M. Chow, "A Network based, Delay-tolerant, Integrated Navigation System for a differential drive UGV using Harmonic Potential Field", Accepted for presentation at: CDC 2006 45th IEEE Conference on Decision and Control December 13-15 2006 Manchester Grand Hyatt San Diego, California USA, pp. 1870-1875.

[21]A. Masoud, "An Informationally-Open, Organizationally-Closed Control Structure for Navigating a Robot in an Unknown, Stationary Environment" 2003 IEEE International Symposium on Intelligent Control, October 5-8, 2003, Houston, Texas, USA, pp. 614-619.

[22] J. Jackson , "Classical Electrodynamics", Wiley, 1989

[23] N. Lawrance, S. Sukkarieh, "A guidance and control strategy for dynamic soaring with a gliding UAV", 2009 IEEE International Conference on Robotics and Automation Kobe International Conference Center Kobe, Japan, May 12-17, 2009, pp. 3632-3637.

[24]A. Masoud, “Motion Planning with Gamma-Harmonic Potential Fields”, to appear in the IEEE Transactions on Aerospace Systems.

[25] A. Masoud, “A Virtual Velocity Attractor, Harmonic Potential Approach for Joint planning and control of a UAV”, 2011 American Control Conference on O'Farrell Street, San Francisco, CA, USA June 29 - July 01, 2011, pp. 432-437.

[26] A. Masoud, “A Harmonic Potential Approach for Simultaneous Planning & Control of a Generic UAV Platform”, to appear in: Journal of Intelligent and Robotic Systems (sepcial issue on aerospace systems).